Noisy precursors in one-dimensional patterns

G. Agez, C. Szwaj, E. Louvergneaux, and P. Glorieux
Laboratoire de Physique des Lasers, Atomes et Molécules, UMR CNRS 8523, Centre d'Études et de Recherches Lasers et Applications, Université des Sciences et Technologies de Lille, F-59655 Villeneuve d'Ascq Cedex, France
(Received 29 May 2002; published 12 December 2002)

Noisy pattern precursors have been observed experimentally in a Kerr-like slice subjected to one-dimensional (1D) optical feedback. These noise-induced patterns appear below threshold and anticipate the characteristics of the incoming patterns. In our 1D system, precursors are rolls with an undefined spatial phase which wanders erratically and locks spatially when crossing the threshold. Phase localization allows for a criterion to define the threshold in presence of noise. The experimental observations are well reproduced by the standard model of the Kerr slice medium with optical feedback when Langevin noise terms are included.

DOI: 10.1103/PhysRevA.66.063805 PACS number(s): 42.65.Sf, 47.54.+r, 05.40.−a, 05.45.−a

I. INTRODUCTION

Pattern formation in optical systems has received several waves of interest. First, threshold conditions were derived and the mechanisms through which the patterns, e.g., hexagons or rolls, originate were discussed [1]. Recently, the interplay between the quantum nature of light and pattern formation was explicitly considered [2]. Quantum images were predicted on the basis of models leading to Fokker-Planck type of equations or to stochastic equations equivalent to the classical models in which noise terms have been added [3]. On the experimental side, the quantum images are still to be observed. In this context, the influence of classical noise in pattern formation must be cleared out so as to separate the quantum effects from the classical ones.

Indeed, classical noise (e.g., thermal noise) may have nontrivial effects in nonlinear spatially extended systems, such as noise-sustained structures [4] and precursors [5]. Noisy precursors were first observed in temporal dynamical systems where the presence of a period doubling or a Hopf bifurcation may be anticipated in the spectrum of the variables [6]. In spatiotemporal dynamics, noisy precursors correspond to the anticipation, below threshold, of some characteristics (such as the wave number) of the pattern appearing above threshold. For instance, a ring in the Fourier transform (FT) of the pattern amplitude (the far field) is observed below the onset in Rayleigh-Bénard convection [5]. This ring reduces at threshold to six equidistant spots in the case of a hexagonal pattern. Thus, the precursors correspond to a progressive selection of the modulus of the wave vectors whose azimuths become fixed above onset, giving rise to a good criterion for the localization of the onset. However, in transverse one-dimensional (1D) systems, such a transition may not be observed since roll patterns are characterized by two spots in the far field both below and above the threshold. Such rolls were observed in a 1D electroconvection system by Rehberg [7] with a fluctuating phase below threshold. These phase fluctuations may be used as a tool to study and characterize 1D noisy precursors.

The purpose of this article is to show that 1D noisy precursors also exhibit localization in a suitable representation and to propose a reliable criterion for ''threshold location'' in 1D optical pattern forming systems in presence of classical noise. We consider here 1D optical systems in which roll patterns build up above threshold in a supercritical bifurcation. Below threshold and in presence of thermal classical noise, rolls progressively develop with a spatial phase which largely fluctuates. These precursors appear through two peaks at the corresponding wave number in the Fourier space, but in 1D contrarily to the 2D case there is no qualitative change in the far field as the threshold region is crossed. We experimentally show here that threshold is then characterized by the spatial phase localization in the complex Fourier space of the associated pattern.

II. EXPERIMENTAL SETUP

The experiments have been carried out in a Kerr slice medium subjected to optical feedback. It essentially consists in a nematic liquid-crystal (LC) layer irradiated by a strong laser beam which is reflected back onto the sample by a simple plane mirror placed at a variable distance from the LC layer. The reorientation of the LC director by the laser electric field leads to a nonlinear change of its refractive index. This setup mimics the Kerr slice with feedback proposed by Firth for optical pattern formation [8]. The first bifurcation that occurs in this system is a transition between the homogeneous state and a space ordered state where rolls or hexagons appear as experimentally observed by Macdonald and Danlewski [9], and Tamburrini *et al.* [10], respectively. Noise originates here from thermal fluctuations which induce random motion of the molecular axis around the mean director azimuth, leading to local variations of the birefringence in the LC.

In our experiments, Fig. 1, the nonlinear medium is a 50-μm-thick layer of E_7 LC homeotropically anchored. This LC sample is placed inside the beam delivered by a single-mode frequency doubled $Nd^{3+}:YVO_4$ laser ($\lambda_0 = 532$ nm) which has been shaped by means of two cylindrical telescopes. The resulting diameters ($\approx 200\mu m \times 2800\mu m$) of the ''cigar'' transverse laser beam differ by a factor of 14 in the vertical (y) and horizontal (x) directions. The smallest waist (e.g., vertical) is chosen such that only one roll can develop in its direction and the system may be considered as monodimensional. After passing through the LC layer, the light is reflected back by an optical system made of two lenses and a

 ©2002 The American Physical Society

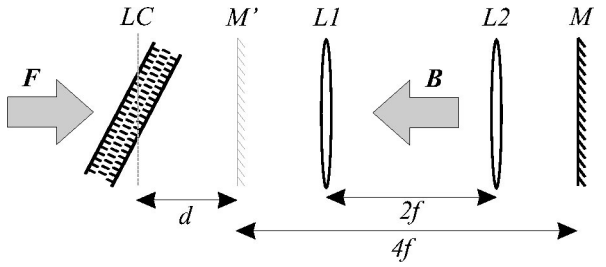

FIG. 1. Experimental setup; LC liquid crystal layer; L_1, L_2 lenses of focal length f; $M\,(M')$ real (virtual) feedback mirror; F, B forward and backward optical fields.

plane mirror in a $4f$ arrangement. This optical setup is equivalent to a fictitious mirror placed at an adjustable distance d from the LC sample where d may be positive or negative. Note that the equivalent medium is self-focusing (defocusing) if $d>0$ $(d<0)$ [11]. The reflected beam is monitored after its second passage through the LC layer. Near and far fields are simultaneously recorded. Two control parameters are easily accessible in the experiments, namely, the maximum intensity I_0 of the incident laser beam and the distance d between the fictitious mirror and the LC layer.

III. EXPERIMENTS

We first study how the patterns appear near threshold in the presence of noise. In our operating conditions, aspect ratio $\eta \approx 37$ [12] ($d=-10$ mm, waist $w_x=1400$ μm), this corresponds to incident intensity varying from 95 to 210 W/cm^2. Beneath this range, the transverse profile of the transmitted beam is almost homogeneous and simply reflects the Gaussian dependence of the incident beam. Beyond it, secondary instabilities appear which are not discussed here [13]. The near threshold region exhibits two distinct regimes, a ''wandering'' and a ''stationary'' one. The latter, observed above threshold [14], corresponds to stationary fringes which are the optical 1D manifestation of the standard roll pattern [Fig. 2(c)]. The wandering regime is observed in the intensity domain between the homogeneous state and the stationary rolls making the transition continuous. This last regime is characterized by rolls with a wave number similar to that of the stationary pattern obtained at higher power, but with a

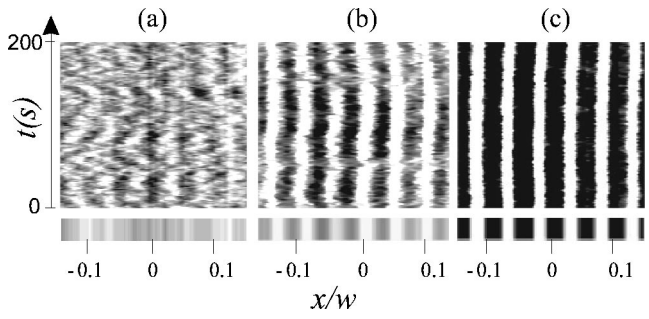

FIG. 2. Evolution of the roll patterns in the near threshold region for different values of the incident intensity I_0 (a) 130 W/cm^2, (b) 170 W/cm^2, and (c) 205 W/cm^2. Vertical axis, time; horizontal axis, space. The lower rectangles represent averages over 500 s.

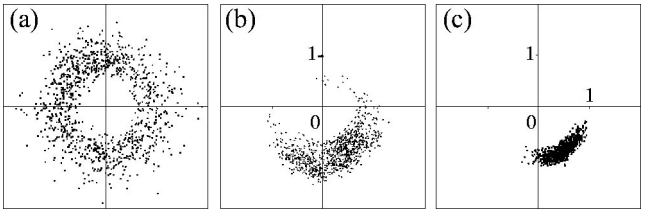

FIG. 3. Complex plane plot of the Fourier-transform component $I_{q_0}(t)$ of the transmitted intensity for different values of the incident laser power (a) 130 W/cm^2, (b) 170 W/cm^2, and (c) 205 W/cm^2. Duration 500 s with a time interval 0.5 s. The amplitudes have been normalized to the average value.

fluctuating spatial phase [Figs. 2(a), 2(b)]. The transition between this regime and the stationary one is accompanied by a progressive locking of the spatial phase (Fig. 2). As it will be demonstrated by numerical simulation, the fluctuating phase is related to the presence of noise in the system, and therefore the wandering rolls are the noisy *precursors* of the incoming pattern.

The existence of the precursors is clearly exhibited using the FT of the near field intensity $I(x,t)$. This has been performed on four rolls in the central part of the pattern to select a range of almost constant input power I_0 $(\Delta I_0/I_0<10^{-2})$ in order to assume almost space-independent wave number q and phase φ. Above threshold the spatial FTs of the transmitted intensity $I(q,t)$ exhibit a large and sharp peak centered at q_0. This peak is the Fourier signature of the rolls. Its modulus $\mathcal{I}_{q_0}$ decreases as the incident power is reduced but it is still quite visible in the region of the wandering rolls, e.g., at an incident intensity of 100 W/cm^2. We concentrate on the evolution of the FT component at the corresponding spatial frequency q_0 through the variables $\mathcal{I}$ and φ of the transverse modulation $I_{q_0}(t)=\mathcal{I}_{q_0}(t)\exp[i\varphi_{q_0}(t)]$ (we leave out q_0 in the following). The standard representation uses two traveling waves whose amplitudes fluctuate independently below threshold. In our experiments we use the Fourier plane representation which is equivalent but best suited since we shall see the behavior of the amplitude and the phase separately in the near threshold region.

On Fig. 3, we have plotted in the complex plane, the real and imaginary parts of $I(t)$ for different values of the incident power. In this diagram, each point is represented in polar coordinates by $(\mathcal{I},\varphi)$. Two qualitatively different dynamical behaviors are observed: (i) well below threshold [Fig. 3(a)], the FT gives a cloud of points centered around zero, indicating the absence of order at this wavelength, the phase φ randomly fluctuates within 2π, (ii) well above threshold [Fig. 3(c)], i.e., when the roll pattern is stationary, the points cluster in a zone whose size is fixed by the noise level. These two regimes are connected by the noisy precursors domain where the point distribution shrinks progressively as the incident power increases [Fig. 3(b)]. The points progressively cluster in a crescent revealing progressive phase and amplitude localization. Note that the average angle of the clusters displayed in Figs. 3(b) and 3(c) is pinned by the boundary conditions and particularly by the Gaussian profile of the pump intensity. Measurements remain consis-

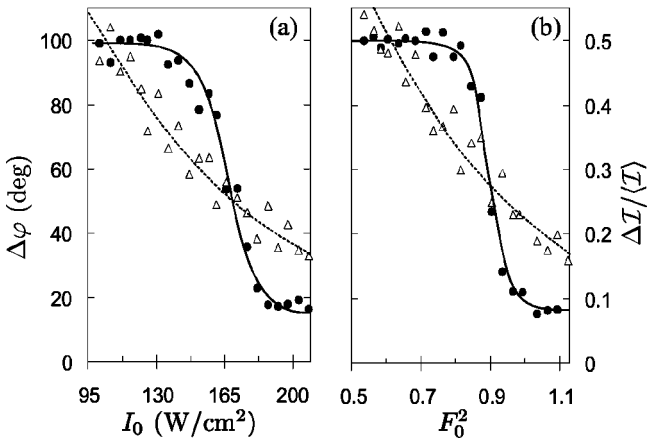

FIG. 4. Dependence vs input intensity of the phase standard deviation $\Delta\varphi$ (black filled circles) and of the relative amplitude standard deviation $\Delta\mathcal{I}/\langle\mathcal{I}\rangle$ (triangles) in the near threshold region (a) experiments, (b) numerical simulations.

tent for total recording times in the 10–500 s range.

We evaluate the phase and relative amplitude spread by plotting the evolution of their standard deviations ($\Delta\varphi$ and $\Delta\mathcal{I}/\langle\mathcal{I}\rangle$) near the threshold [Fig. 4(a)]. The curve obtained for $\Delta\varphi$ clearly evidences the two dynamical behaviors ($\Delta\varphi \approx 100°$ and 20°) previously mentioned. The first one corresponds to a uniform distribution ($\Delta\varphi = 104°$) of the phase, indicating that the phase can take any value within 360°. The second one corresponds to the stationary rolls. The interesting feature is that these two regimes are well separated by a rather sharp transition of $\Delta\varphi$ near 165 W/cm^2 (or 0.95 W). By comparison, the curve of the roll amplitude standard deviation $\Delta\mathcal{I}/\langle\mathcal{I}\rangle$ is very much smoother [Fig. 4(a)]. The plot of the wave-number q_0 evolution shows that its mean value remains constant throughout the observed range. Thus, the roll precursors have already the ''good'' wave number but no definite phase. The spatial phase localization is the 1D counterpart of the azimuthal phase locking in the 2D systems.

IV. NUMERICAL SIMULATIONS

Our results have been compared with numerical simulations on the basis of the equations proposed by Firth for a Kerr slice medium with a single feedback mirror [8]. Thermal fluctuations in the LC are modeled by adding a Gaussian white-noise term $\xi(x,t)$ in the medium refractive index $n(x,t)$ equation which reads in adimensional form,

$$-\frac{\partial^2}{\partial x^2}n+\frac{\partial n}{\partial t}+n=|F|^2+|B|^2+\sqrt{\varepsilon}\,\xi$$

with

$$B=\sqrt{R}e^{i\sigma(\partial^2/\partial x^2)}e^{i\chi n}F.$$

F is the forward input optical field, its Gaussian transverse profile is taken into account by using $F(x) = F_0\exp(-x^2/w^2)$, where w is the beam radius at sample position. B is the backward reflected field and R is the mirror reflectivity. The noise is scaled by ε and χ parametrizes the Kerr effect. $\sigma = d/(k_0 l_D^2)$ measures the diffraction to diffusion ratio, where d is the optical feedback length, $k_0 = 2\pi/\lambda_0$ is the laser wave number and l_D is the diffusion length of the liquid crystal (which is ≈ 8 μm in our system [15]). The spatial variables are scaled with respect to l_D and the time to the relaxation time (of the order of the second). A standard procedure has been used for integrating the stochastic equations [16]. The experimental observations are well reproduced by numerical simulations for $\sigma = -10$, $w = 200$, and F_0^2 between 0.5 and 1.1 typically. If no noise is injected in the model ($\varepsilon = 0$), we can determine the exact threshold value ($F_0^2 = 0.9$). Below this value no pattern is observed. However if noise is added ($\varepsilon = 10^{-2}$), below threshold, e.g., $F_0^2 = 0.79$, rolls with clear contrast are observed at any time as in the experiments.

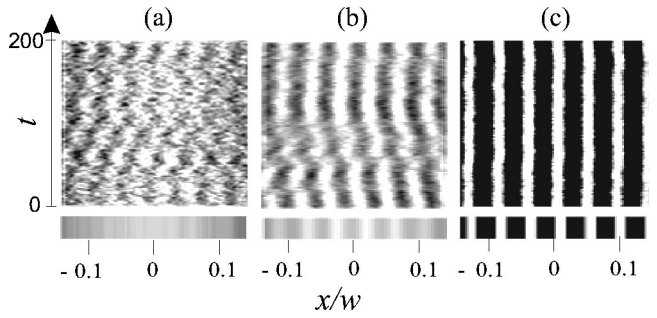

FIG. 5. Numerical simulations with parameters $\chi = 1$, $\sigma = -10$, $R = 0.9$, $\eta = 35$, $F_0 = 0.79$ (a), 0.9 (b), and 1.09 (c). Vertical axis, time. Horizontal axis, space. Lower rectangles represent averages of 500 time units.

As shown on Fig. 5(a), when time goes on, they experience random translational jumps. For higher F_0^2 (1.05), the spatial phase locks and the pattern becomes stationary [Fig. 5(c)]. The evolution of these patterns is still characterized by the localization property of their spatial phase and amplitude. A steeper transition is observed for the phase as compared to the amplitude standard deviation as shown on Fig. 4(b). More quantitatively, the noise amplitude $\varepsilon = 10^{-2}$ was chosen to match the experiments by measuring the steepness of the transition of $\Delta\varphi$. The larger the noise, the wider the transition. Thus, the comparison between experiments and simulations can serve to measure the noise parameter, assuming that experimental noise statistics follow the standard distribution for thermal effects.

V. DISCUSSION

Numerical simulations allow us to compare the system with and without noise, the latter giving access to the noiseless threshold value ($F_0^2 = 0.9$). We can then discuss about the value of this threshold as compared to the phase localization transition location or else the threshold obtained from amplitude (of modulation) versus F_0. Indeed, the relatively sharp transition of the phase spread may be used to redefine the threshold in presence of noise as, e.g., the onset of phase coherence in the system. In the case of Fig. 5, the inflexion point of the $\Delta\varphi$ curve is measured at 0.895 which is very

close to the threshold value in the absence of noise. Fits carried out on amplitude $\mathcal{I}$ evolution versus control parameter F_0^2 give values from 0.85 to 0.95 depending on the fitting and averaging procedures. We have checked that this criterion for finding the threshold is robust with respect to changing the sampling and recording times.

VI. CONCLUSION

In conclusion, the investigation of the onset of pattern formation in a 1D system reveals the existence of noisy precursors. They correspond to an emerging periodic pattern with a preferred wavelength equal to that of the rolls observed above threshold but these rolls experience random translational jumps. A Fourier analysis indicates that the crossing of the threshold is characterized by a localization of their transverse spatial phase that locks above threshold. This transition that coincides with the crossing of the threshold suggests a criterion for threshold location in noisy systems. This buildup of 1D noisy precursors is somehow the analog in the complex plane of the progressive localization of 2D precursors in the real space plane, more precisely in the far-field transform in real space [5]. Our experimental observations are in good agreement with a model in which a classical noise term has been introduced and therefore can be used to scale noise in experimental systems. All these classical noise-induced phenomena must be considered in future work on quantum images which investigate the effect of quantum noise on patterns.

ACKNOWLEDGMENTS

We would like to thank M. San Miguel, P. Colet, P. Scotto, and M. Taki for useful discussions. The Laboratoire de Physique des lasers, Atomes et Molecules is Unité de Recherche Mixte du CNRS. The Center d'Études et de Recherches Lasers et Applications was supported by the Ministère chargé de la Recherche, the Région Nord-Pas de Calais, and the Fonds Européen de Développement Économique des Régions.

[1] L.A. Lugiato, Phys. Rep. **219**, 293 (1992).
[2] A. Gatti and L. Lugiato, Phys. Rev. A **52**, 1675 (1995).
[3] A. Gatti, H. Wiedemann, L.A. Lugiato, I. Marzoli, G.-L. Oppo, and S.M. Barnett, Phys. Rev. A **56**, 877 (1997).
[4] M. San Miguel and R. Toral, *Stochastic Effects in Physical Systems* (Kluwer Academic, Dordrecht, 2000).
[5] M. Wu, G. Ahlers, and D.S. Cannell, Phys. Rev. Lett. **75**, 1743 (1995).
[6] C. Jeffries and K. Weisenfeld, Phys. Rev. A **31**, 1077 (1985); K. Wiesenfeld, *ibid.* **32**, 1744 (1986); P. Pieranski and J. Malecki, *ibid.* **34**, 582 (1986).
[7] I. Rehberg, S. Rasenat, M. de la Torre Juárez, W. Schöpf, F. Hörner, G. Ahlers, and H.R. Brand, Phys. Rev. Lett. **67**, 596 (1991).
[8] W.J. Firth, J. Mod. Opt. **37**, 151 (1990); W.J. Firth and G.P. D'Alessandro, Phys. Rev. Lett. **66**, 2597 (1991).
[9] R. Macdonald and H. Danlewski, Opt. Lett. **20**, 441 (1995).
[10] M. Tamburrini, M. Bonavita, S. Wabnitz, and E. Santamato, Opt. Lett. **18**, 855 (1993).
[11] E. Ciaramella, M. Tamburrini, and E. Santamato, Appl. Phys. Lett. **63**, 1604 (1995).
[12] The aspect ratio η corresponds to the ratio of the beam diameter to the theoretical roll wavelength calculated in a uniform configuration. It measures the transverse size of the system.
[13] E. Louvergneaux, Phys. Rev. Lett. **87**, 244501 (2001).
[14] At this point it is difficult to define rigorously a ''threshold.'' However in experiments, a threshold region as defined by the emergence of ''almost stationary'' rolls is easily located within 10%. In simulations, threshold is used by reference to the noiseless situation keeping in mind the continuous transition in presence of noise.
[15] E. Santamato, E. Ciaramella, and M. Tamburrini, Mol. Cryst. Liq. Cryst. **251**, 127 (1994).
[16] M. Neufeld, D. Walgraef, and M. San Miguel, Phys. Rev. E **54**, 6344 (1996).